Earth and Planetary Science Letters 430 (2015) 448–457

Contents lists available at ScienceDirect

Earth and Planetary Science Letters

www.elsevier.com/locate/epsl

Knickpoint evolution on the Yarlung river: Evidence for late Cenozoic uplift of the southeastern Tibetan plateau margin

Jennifer L. Schmidt [a,*], Peter K. Zeitler [a], Frank J. Pazzaglia [a], Marissa M. Tremblay [b,c], David L. Shuster [b,c], Matthew Fox [b,c]

[a] Department of Earth and Environmental Sciences, Lehigh University, 1 W. Packer Ave., Bethlehem, PA 18015, USA
[b] Department of Earth and Planetary Science, University of California, Berkeley, 307 McCone Hall #4767, Berkeley, CA 94720-4767, USA
[c] Berkeley Geochronology Center, 2455 Ridge Road, Berkeley, CA 94709, USA

ARTICLE INFO

Article history:
Received 1 May 2015
Received in revised form 25 August 2015
Accepted 31 August 2015
Available online xxxx
Editor: M. Bickle

Keywords:
Yarlung river
landscape evolution
knickpoint celerity modeling
^{4}He/^{3}He apatite thermochronology
thermokinematic modeling

ABSTRACT

A salient geomorphic feature of the Yarlung River is its abundance of large knickpoints, which in many cases coincide with north–south trending rifts. Across one of these rifts, near the town of Jiacha, the Yarlung falls nearly 500 m from an elevation of ~3500 m over 80 river kilometers, making this the second largest knickpoint on the river. We propose that the Jiacha knickpoint represents a wave of incision migrating upstream through the drainage network in response to a downstream base level fall, not a disturbance in the channel to due rift tectonics.

Longitudinal profile slope-area and chi (χ) analysis of Yarlung River tributaries and those of several major rivers in southeastern Tibet indicate several knickpoints are present at ~3500 m elevation, all resulting from a single regional-scale base level fall. Retreat rates calculated from celerity modeling indicate that the Jiacha knickpoint was located at the upstream edge of the Namche Barwa massif at ~10 Ma, a history consistent with apatite ^{4}He/^{3}He thermochronometry data and thermokinematic modeling from that region. These data suggest the Yarlung River has flowed in its present course through this area since at least 10 Ma and imply that at least 500 m of incision occurred within this canyon over this time period. The spatial scale of these observations suggests that these knickpoints resulted from surface uplift of southeastern Tibet of 500 to 2500 m just prior to ~10 Ma. Additionally, our mapped knickpoint locations indicate that reorganization of the drainage network just east of the Namche Barwa massif occurred prior to this time.

1. Introduction

The Yarlung River flows strike parallel to the Himalayan orogen for ~1700 km in southern Tibet before it abruptly drops over an ~2 km knickpoint and changes trajectory by ~180° in a gorge only 200 km long in the eastern Himalayan syntaxis (Fig. 1). The river drains >200,000 km^2 of the Tibetan plateau and delivers ~2000 m^3/s of discharge through the syntaxis (Montgomery et al., 2004), making the Yarlung River one of the major drainage catchments in Tibet and the largest in the southern plateau through which eroded sediments are evacuated. The topographic evolution of the southern Tibetan landscape is thus largely controlled by the base level established on the Yarlung drainage.

The longitudinal profile of the Yarlung River contains several large knickpoints, river reaches with convex elevation profiles and anomalously steep slopes (Fig. 2A). In the eastern portion of the catchment, near the town of Jiacha, the Yarlung channel navigates a narrow bedrock gorge, falling ~500 m in elevation over 80 river km from an elevation of 3500 m to form the second largest knickpoint on the river. In a detachment-limited stream power model (Howard and Kerby, 1983; Howard, 1994; Whipple and Tucker, 1999), in which elevation is increased due to rock uplift rate (U) and lowered through erosion ($E = KA^mS^n$: where A is upstream drainage area; S is local along channel slope; K is bedrock erodibility), such deviations from a graded, concave-up profile in a long-lived river imply either spatial variations in rock uplift rate or transience in the system associated with major changes in base level and upstream migration of erosional waves. As with several other knickpoints on the Yarlung River, the Jiacha knickpoint locally coincides with a late Cenozoic N–S trending rift that accommodates E–W extension in southern Tibet (Kapp et al., 2008; Yin et al., 1999; Fig. 1). An obvious inference is that dynamic support and/or active rift-flank uplift is locally steepening the Yarlung channel, forming the knickpoint (Zhang, 1998). However, the lack

* Corresponding author.
E-mail address: jlm711@lehigh.edu (J.L. Schmidt).

http://dx.doi.org/10.1016/j.epsl.2015.08.041
0012-821X/

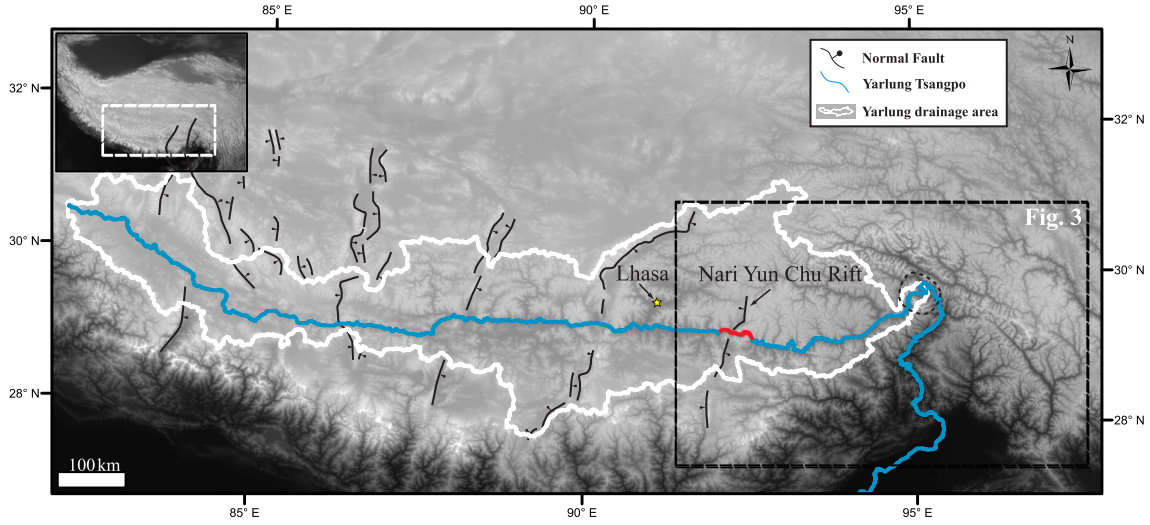

Fig. 1. Overview map of the Yarlung River drainage basin (location highlighted in inset). The drainage area includes a significant portion of southern Tibet. Major rifts (from Kapp and Guynn, 2004) locally coincide with knickpoints along the river. The Nari Yun Chu Rift coincides with the Yarlung River at the Jiacha knickpoint (highlighted in red). Dashed ellipse illustrates approximate area of rapid rock uplift in the Namche Barwa massif (adapted from Stewart et al., 2008). (For interpretation of the references to color in this figure legend, the reader is referred to the web version of this article.)

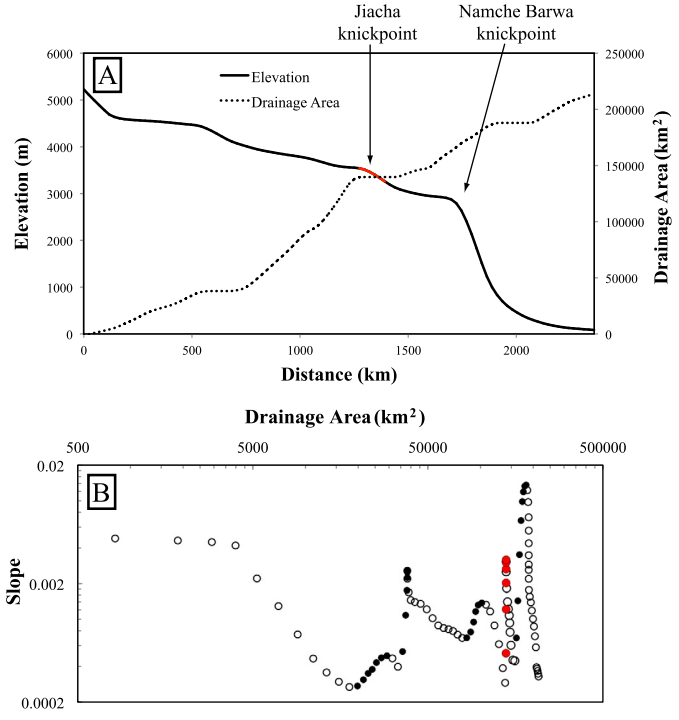

Fig. 2. A) Elevation, drainage area, and SL index plotted against river distance for the Yarlung River. B) Slope-area plot for Yarlung River. Filled circles denote knickpoint reaches. Both A and B highlight the magnitude of the Jiacha (in red) and other knickpoints on the Yarlung River. (For interpretation of the references to color in this figure legend, the reader is referred to the web version of this article.)

of major offset on this rift (Yin et al., 2010) precludes pinning of the Jiacha knickpoint to this location for an extended period of time. An alternative hypothesis that we test here is that the Jiacha knickpoint formed as a result of a regional base level fall downstream of its present position, propagating through the drainage network and triggering a wave of incision that is presently carving through the eastern Jiacha rift flank. Knickpoints originating in this manner travel upstream with a celerity of KA^m (assuming $n = 1$; Crosby and Whipple, 2006; Rosenbloom and Anderson, 1994; Weissel and Seidl, 1998; Whipple and Tucker, 1999; Whipple et al., 2000) and should be evident in rivers throughout the drainage network. Furthermore, solutions to the stream power model indicate that transient features with a constant travel time (τ) should be present at the same elevation (Weissel and Seidl, 1998; Pritchard et al., 2009; Royden and Perron, 2013; Goren et al., 2014). As there is no signature of K within the landscape, it is possible to calculate a K-independent travel time with units of length (Perron and Royden, 2013), termed χ, where $\chi(x) = KA_0^m \tau(x)$. By this method, knickpoints are identified at a specific elevation and corresponding χ value. These represent idealized scenarios and in reality, U and K can be spatially and temporally variable due to complex tectonics or variations in lithology or climate, respectfully. Nevertheless, this simplified stream power model provides a framework to assess the origin of this knickpoint, its relationship to knickpoints of similar elevation in southeastern Tibet, and implications for late Cenozoic drainage reorganization and landscape evolution.

We test these ideas through a combination of longitudinal profile and knickpoint celerity modeling, ^{4}He/^{3}He apatite thermochronometry, and thermokinematic modeling to constrain the Cenozoic incision history of the Yarlung downstream of the Jiacha knickpoint. Our results provide new perspective on the timing of river capture east of the eastern Himalayan syntaxis. We highlight the integration of knickpoint mapping with ^{4}He/^{3}He apatite thermochronometry and thermokinematic modeling as a novel approach to interpreting paleo-drainage patterns. Finally, we speculate on the origin of the Jiacha knickpoint by examining river profiles throughout eastern Tibet.

2. Identifying transient features in the Yarlung drainage network

We analyzed longitudinal profiles of the Yarlung and its tributaries upstream of the Namche Barwa massif to document evidence for migration of the Jiacha knickpoint in the reach immediately downstream, where knickpoint preservation is most likely. We used a 30 m ASTER digital elevation model (DEM) of southern Tibet as our base data set downloaded from the USGS Global Data Explorer (gdex.cr.usgs.gov/gdex). Using ESRI ArcGIS software, we extracted longitudinal elevation and drainage area profiles of the Yarlung and several of its tributaries, smoothing profiles using a loess filter in order to decrease noise and highlight the general form of the profile.

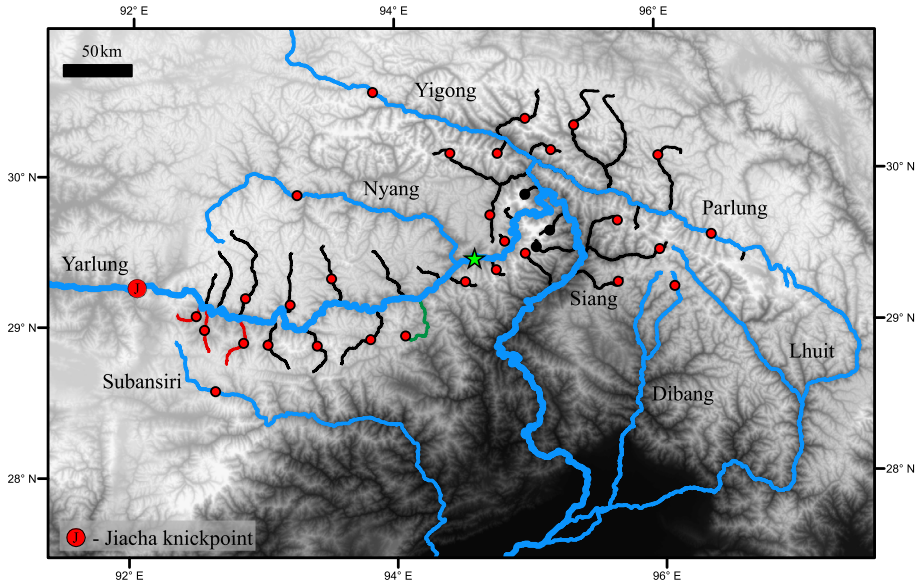

Fig. 3. Analyzed tributaries (black, red, and green) and major rivers (blue) of southeastern Tibet (location highlighted in Fig. 1). Circles indicate locations of identified knickpoints at ~3500 m elevation. Black circles indicate reaches with convex profiles that are not associated with fluvial knickpoints (see Section 2). Tributaries used in knickpoint celerity modeling are highlighted in red. Green tributary has undergone a recent capture event as discussed in Section 2 and Fig. 4B. Green star indicates the projected Jiacha knickpoint location at ~10 Ma, based on our knickpoint celerity model. (For interpretation of the references to color in this figure legend, the reader is referred to the web version of this article.)

As erosion rate in the stream power model is equal to KA^mS^n, assuming the river is in steady state, erosion rate is equal to uplift rate ($U = KA^mS^n$) and we can therefore gain insight into relative erosion rates by analyzing the relationship between S and A. This is achieved by rearranging this expression and regressing linear segments of the streams in $\log S$–$\log A$ space to provide a channel steepness index ($k_s = [U/K]^{1/n}$) and concavity ($\theta = m/n$). This slope-area analysis objectively highlights knickpoints in the profile (Hack, 1957; Kirby and Whipple, 2001; Snyder et al., 2000). We identified knickpoints where there is a change in a linear array of values to negative concavity in $\log S$–$\log A$ space, i.e. where a particular reach has a convex profile (Fig. 2B).

37 notable knickpoints exist within the Yarlung and 18 of its tributaries in the reach between the Namche Barwa massif and Jiacha knickpoint (Fig. 3). One of these knickpoints coincides with a mapped lithologic boundary. Of the others, 13 occur at elevations of $3500 \pm \sim 150$ m, the approximate elevation of the Jiacha knickpoint. The lithology of the tributaries north of the Yarlung is more variable than that of the southern tributaries and those lacking knickpoints at ~3500 m are focused in the north. This additional lithologic variation likely stalled or enhanced headward migration of these northern knickpoints, affecting their elevation. Cross-valley profiles from above and below the tributary knickpoints do not significantly differ, indicating the common elevation of these features does not reflect a regional erosive process change from fluvially dominated to glacially dominated at ~3500 m elevation. The morphology of this landscape at or below this elevation is therefore not controlled by glacial erosion.

A strong correlation exists between drainage area upstream of these 13 knickpoints and their distance from tributary confluence with the Yarlung (Fig. 4A). Since the celerity of knickpoint retreat in the stream power model is proportional to the drainage area raised to the power of m, this drainage area dependence on the horizontal distance a knickpoint will travel predicts this relationship when knickpoints are the result of a common base level fall (Berlin and Anderson, 2007; Goren et al., 2014; Harkins et al., 2007; Niemann et al., 2001; van der Beek and Bishop, 2003; Whipple and Tucker, 1999; Zaprowski et al., 2001). We can further investigate this relationship by looking for commonalities across entire tributary channels and not solely the knickpoints. To remove the dependence of drainage area and negate the need to calculate slopes, as those derived from DEMs are prone to noise, we calculate χ-elevation profiles for the Yarlung River and its tributaries (Perron and Royden, 2013). If the tributaries share a common base level history they should overlap in χ-elevation space. Divergence of the profiles may be due to spatial variation in channel incision processes or non-uniform precipitation expressed in K (Perron and Royden, 2013). For the Yarlung and its tributaries, steps corresponding to knickpoints at ~3500 m elevation exhibit significant overlap, suggesting that these knickpoints are the result of a single, downstream base level fall. The dissimilarity in the overall morphology of the χ-elevation profiles between the northern and southern tributaries may result from a difference in hillslope and fluvial erosion processes arising from aspect and/or rock type.

The profile in Fig. 4B shown in green contains a knickpoint at ~3500 m; however this profile has significantly different χ values for a given elevation, likely due to recent capture by that tributary as suggested by its anomalous morphology observable in the DEM (see Fig. 3 for tributary location). This indicates that a substantial change in the drainage area occurred after the knickpoint migrated into the area, which increased χ values along this tributary. It is important to note that the absolute χ values are insignificant here given the uncertainty in the magnitude of the total elevation change across the Jiacha knickpoint (see Section 6.3). Placing time constraints on the age of these knickpoints and commonalities requires external data and is discussed in Section 3.

The detection of downstream knickpoints within streams east of the Namche Barwa massif provides possible tests for mechanisms for this base level fall. Longitudinal profiles from six tributaries in the Siang River, along with the Yigong and Parlung rivers and 11 of their tributaries extracted from a 90 m SRTM DEM (downloaded from http://www.viewfinderpanoramas.org) highlight fourteen knickpoints occurring at 3500 ± 200 m (Fig. 3). Three of these knickpoints are located in the Namche Barwa massif within currently glaciated valleys. Longitudinal profiles from these tributaries thus do not reflect the valley bottom profile, but rather a combination of the glacier surface at high elevations and the valley bottom at lower elevations. They are therefore not related to the Ji-

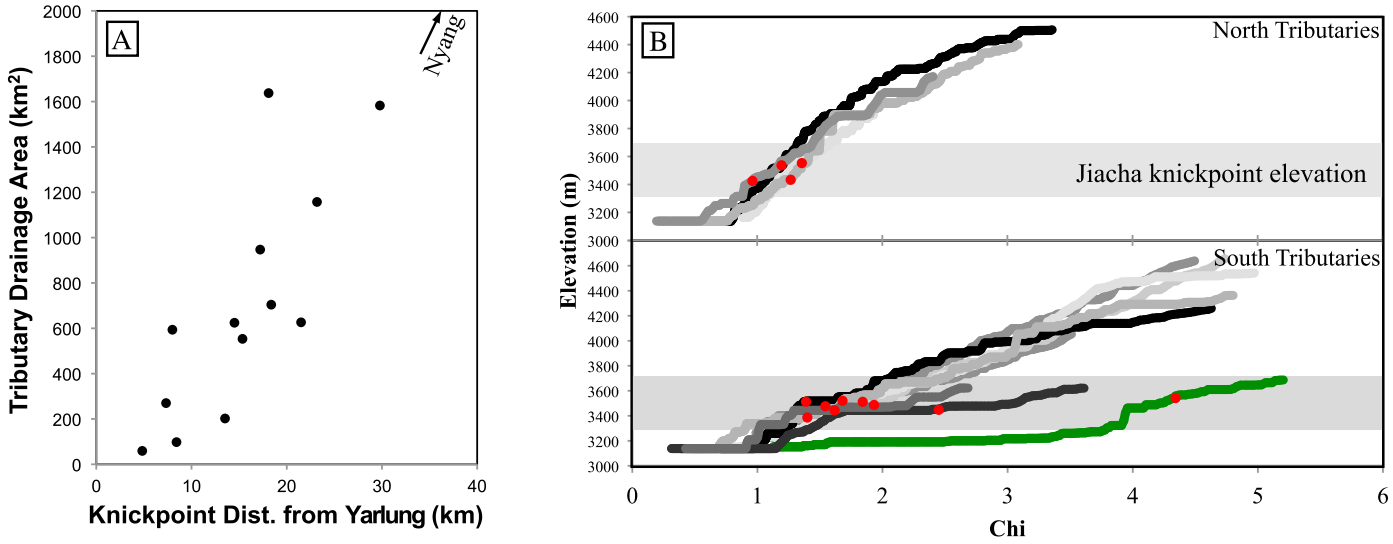

Fig. 4. A) Knickpoint distance plotted against tributary drainage area for Yarlung tributaries containing knickpoints at ~3500 m elevation. Each knickpoint is plotted as filled circle. Note: Nyang river knickpoint located out of plot range. B) χ-elevation plot for tributaries on the north (top) and south (bottom) side of the Yarlung containing knickpoints at ~3500 m (red circles). We assume a concavity of 0.5. South tributary shaded in green (see Fig. 3 for location) displays clear offset in χ, resulting from recent river capture as discussed in Section 2. (For interpretation of the references to color in this figure legend, the reader is referred to the web version of this article.)

acha knickpoint. Major rivers analyzed draining the eastern plateau margin and the Himalaya including the Subansiri, Dibang, Lhuit, Irrawaddy, Salween, Mekong, Yangtze, and Yalong (Fig. S1) also have knickpoints at ~3500 m, with the exception of the Lhuit (Fig. 3). We discuss the implications of common elevation knickpoints in drainage networks spanning such a large area in Sections 6.2 and 6.3.

3. ^{3}He/^{3}He apatite thermochronometry

The development of high-relief topography such as that observed within the Yarlung River valley will perturb shallow crustal isotherms and thus shape the thermal history of the valley (Mancktelow and Grasemann, 1997; Braun, 2002). If a wave of sufficiently deep incision migrated headward along the Yarlung River, bedrock downstream of Jiacha should record exhumation-related cooling associated with passage of the knickpoint. Apatite ^{4}He/^{3}He thermochronometry constrains cooling histories through the uppermost few km of the crust. Schildgen et al. (2010) and Shuster et al. (2011) have demonstrated the potential of this method in identifying incision propagating through high-relief valleys. Here, we apply the method to samples downstream of the Jiacha knickpoint.

Retention of radiogenic ^{4}He, produced by alpha decay of U, Th, and Sm begins below ~85 °C and is complete by ~30 °C in apatite, depending on the size, cooling path, and the U, Th, and Sm concentrations of a given apatite crystal (Flowers et al., 2009; Shuster et al., 2006). A bulk (U–Th)/He apatite age is calculated from the total abundances of ^{238}U, ^{232}Th, ^{147}Sm and radiogenic ^{4}He in an apatite, and provides a non-unique constraint on the timing and rate of cooling between these temperatures. In ^{4}He/^{3}He thermochronometry, stepwise degassing analysis of a sample containing a uniform distribution of proton-induced ^{3}He resolves the spatial distribution of ^{4}He within a crystal, which more restrictively constrains an individual sample's thermal history (Shuster et al., 2004); the ^{4}He distribution and the (U–Th)/He age can thus be used to exclude thermal histories that are permitted on the basis of the (U–Th)/He age alone.

Our topographic analysis predicts that background exhumation within the valley will be punctuated by a period of rapid incision associated with knickpoint migration. If the knickpoint propagated upstream, this transient pulse of incision will have migrated with time. Bedrock apatite (U–Th)/He ages should therefore correlate with downstream distance from the Jiacha knickpoint and ^{4}He/^{3}He modeled thermal histories will provide constraints on the cooling rate. We applied these methods to two sample sets collected within the Yarlung River valley to (1) ascertain the relationship between bedrock age and distance along the river, and (2) use modeled thermal histories to determine if samples experienced a pulse of rapid cooling.

We collected two groups of bedrock samples along the Yarlung River valley bottom (Table S1). The first group was collected near the base of the Jiacha knickpoint, while the second group spans a 100 km transect beginning ~200 km downstream from the lip of the Jiacha knickpoint (Fig. 5). Sample collection at river level maximizes the potential for recording knickpoint migration-induced incision, as these samples would experience the greatest amount of exhumation from this process. For analysis, we selected individual euhedral apatite grains free of visible inclusions and with a spherical equivalent radius of at least 50 μm from each sample. Following methods described by Shuster et al. (2004), samples were subjected to proton irradiation to produce a uniform distribution of ^{3}He. The ^{4}He/^{3}He ratio was measured by mass spectrometry during sequential, stepwise degassing of individual crystals (Table S2). The evolution of this ratio with cumulative ^{3}He release reflects the spatial distribution of ^{4}He within each grain. In these cases, we calculate the (U–Th)/He age from the sum of the ^{4}He released in all steps, and the U, Th, and Sm molar abundances in the same grain, measured by isotope dilution. The finite difference model described by Schildgen et al. (2010) was used to model cooling histories that predict the (U–Th)/He age within one standard error. Histories that satisfy this criterion are scored based on their misfit with the observed ^{4}He/^{3}He ratio evolution of these samples (Schildgen et al., 2010). Modeled histories with mean squared error (normalized to mean ratio uncertainty) of <1.5 represent good fits to our observed ratios (see Schildgen et al., 2010).

Fig. 5 shows observed apatite ^{4}He/^{3}He data, modeled cooling histories, and sample locations with respect to the Jiacha knickpoint (see Fig. S3 for overlaid thermal histories). Within the valley transect, (U–Th)/He ages are 8.8 ± 0.88 Ma at the farthest downstream location and young to 4.4 ± 0.44 Ma ~100 km upstream (Fig. 5 & 6), demonstrating that cooling of these samples occurred earlier downstream than upstream. These data are consistent with a wave of cooling associated with incision propagating upstream as

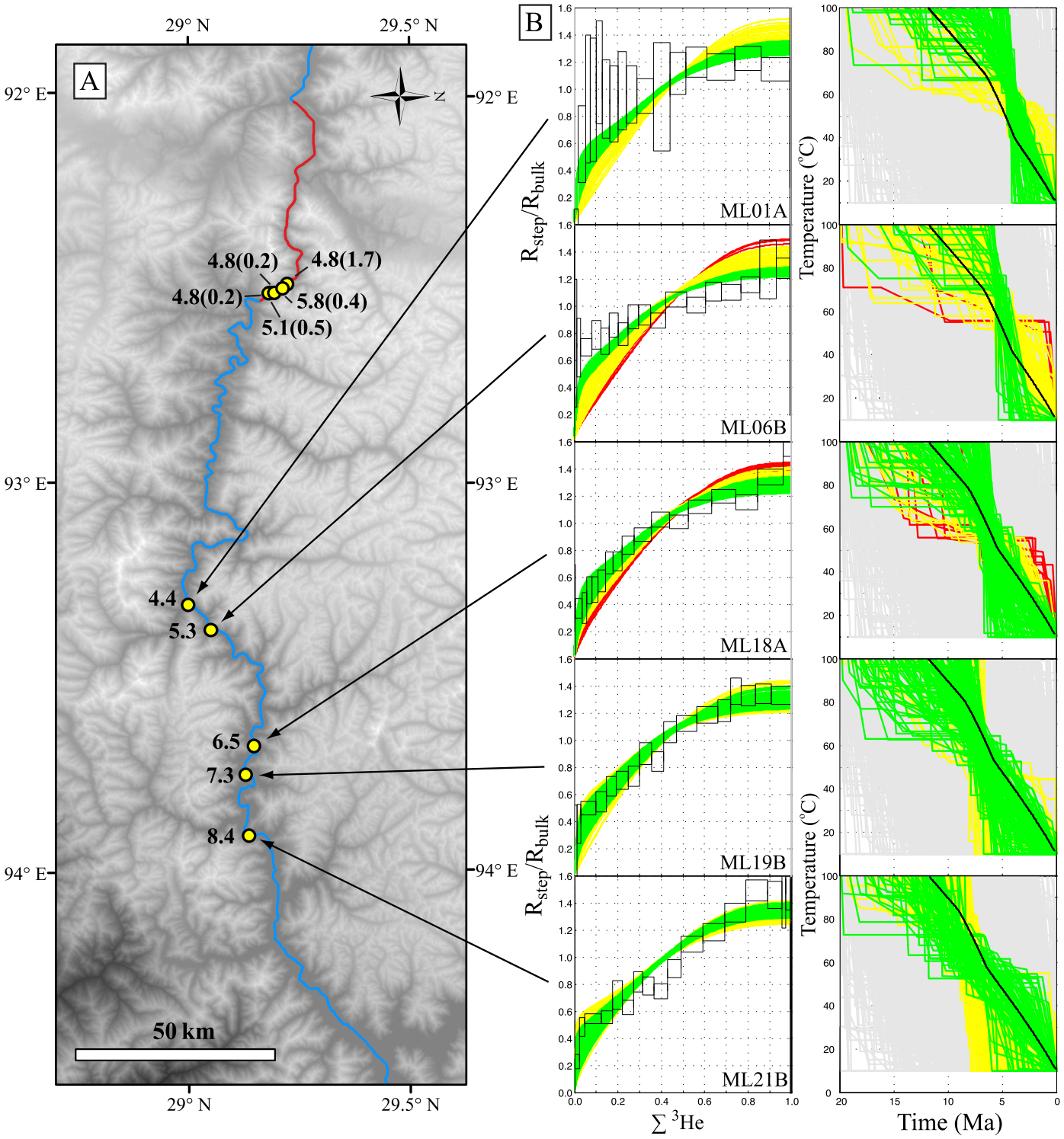

Fig. 5. Sample ages and $^4He/^3He$ results. A) Map showing sample locations (yellow circles) and corresponding (U–Th)/He apatite age. The Jiacha knickpoint is highlighted in red. Samples located at the base of the Jiacha knickpoint are labeled with mean age of all aliquots (shown with 1 standard deviation uncertainty), whereas downstream transect samples are calculated from individual aliquot in shown in B. B) Modeled $^4He/^3He$ time–temperature (right panel) and ratio evolution spectra (left panel) results. Ratios of $^4He/^3He$ for each step relative to the bulk $^4He/^3He$ of a sample are plotted against the cumulative ^3He release fraction ($\sum^3He$; black boxes). Gray paths represent modeled cooling histories that do not predict the sample (U–Th)/He age to within analytical error. Green paths are those that predict the (U–Th)/He age and have good fits to the observed spectra for that sample. Yellow and red paths also predict the age but have progressively worse fits. Black paths are the best fitting of the explored Pecube models. (For interpretation of the references to color in this figure legend, the reader is referred to the web version of this article.)

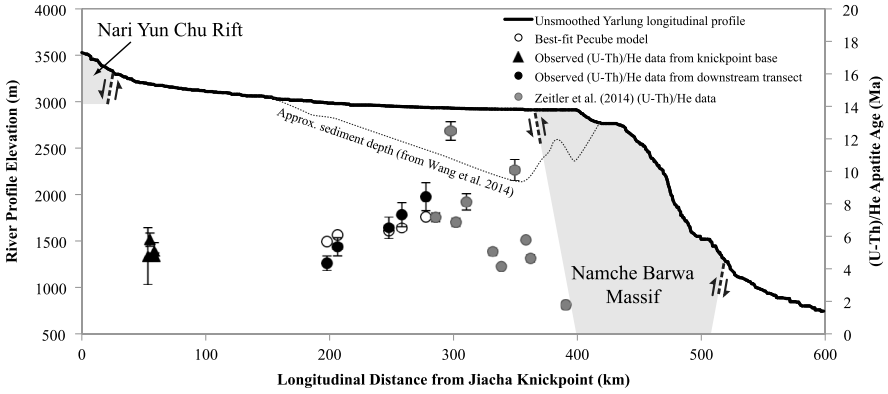

Fig. 6. Apatite (U–Th)/He data from this study plotted with approximate distance from the lip of the Jiacha knickpoint. Open circles are (U–Th)/He age predicted from HeFTy using thermal histories of corresponding sample nodes extracted from the best fitting of the explored Pecube models (see Section 5). Black circles are our observed ^{4}He/^{3}He sample ages from aliquots in Fig. 5 with estimated 10% uncertainty in age. Black triangles are our observed average (U–Th)/He ages with standard deviation for samples from the base of the knickpoint. Gray circles are apatite (U–Th)/He data from Zeitler et al. (2014) and were not included in Pecube model. Approximate sediment depth in Yarlung canyon estimated from Wang et al. (2014).

predicted by our knickpoint model. Apatite (U–Th)/He ages from the base of the knickpoint cluster around 5 Ma. Because of the proximity of these samples to the present-day Jiacha knickpoint, they would have been far above the He partial retention zone (PRZ) when it migrated through this location. We therefore interpret these apatite ages as having been set during pre-knickpoint background erosion.

Thermal histories consistent with the observed ^{4}He/^{3}He data for upstream samples ML01, ML06, and ML18 (Fig. 5, Table S2) do not record a major change in cooling rate but do permit rapid cooling, suggesting they were below or entering the PRZ when knickpoint migration occurred. Because these histories do not record the onset of rapid cooling, we can constrain the timing of initiation of rapid incision at their location only to at least 4 Ma. The samples farthest downstream from the Jiacha knickpoint (ML19, and ML21) display a range of permissible model histories that is broad enough that we cannot resolve if these samples experienced fast or slow cooling. However, rapid cooling related to knickpoint migration by at least 8 Ma is permissible. Collectively, our modeled cooling histories from the valley transect samples constrain a time window (4–8 Ma) over which the samples cooled that young with upstream distance, which is consistent with our model of knickpoint migration. Predicted knickpoint migration rates from these data are 20–25 km/Ma.

In general, ^{4}He/^{3}He data from samples from the base of the knickpoint have uncertainties on the individual heating steps that are too large to provide quantitative constraints. Two samples from this area (LB12-ZD08 and LB12-ZD07) have lower uncertainties; nonetheless we are unable to distinguish between fast and slow cooling histories using these data (Fig. S4). We therefore present mean ages for these knickpoint samples in Fig. 5. Additionally, we conducted conventional single crystal apatite (U–Th)/He analyses, calculating the (U–Th)/He age from the total release of ^{4}He in a single step (Table S3). U, Th, and Sm molar abundances were measured from the same grain by isotope dilution. These ages agree with those determined by ^{4}He/^{3}He thermochronometry for each sample, supporting the trend of decreasing age with distance upstream.

4. Knickpoint celerity modeling

We applied the stream power based knickpoint migration model for the Jiacha knickpoint following the general methodology of Berlin and Anderson (2007) to predict the knickpoint celerity and therefore mean retreat rate of valley incision directly downstream of Jiacha.

We selected three, adjacent north-flowing tributaries directly downstream of the Jiacha knickpoint that have prominent knickpoints at ~3500 m (Fig. 3). Knickpoint celerity modeling is best constrained by using a large number of tributaries that experience instantaneous and coeval base level fall. The Yarlung drainage network geometry makes it difficult satisfy this requirement. Furthermore, differences in rock type among tributaries influence K and differences in aspect influence watershed hydrology (m), as observed in the χ-elevation plot (Fig. 4). For these reasons, solutions to the celerity model that combined north-flowing and south-flowing tributaries resulted in very high residual values for the best-fitting K and m. Although not ideal, the three tributaries used to constrain the celerity model have little to no variation in rock type, are of similar size and hypsometry, and are all confluent with the Yarlung at nearly the same location.

We assumed that these three tributaries experienced a base level fall resulting from Jiacha knickpoint migration at the exact same time, which is reasonable given the proximity of the tributary mouths where they join the Yarlung and the rapid migration rate expected. We modeled m and K values assuming the three tributary knickpoints initiated at 4.4 Ma (t) based on the tributary locations and our interpretation of sample ML01, the closest sample affected by knickpoint-related cooling. The distance from a tributary mouth to the top of the 3500 m elevation knickpoint (x) and the corresponding upstream drainage area for a tributary channel reach (A) are known.

Using the celerity equation, we calculate a travel time through each cell of the tributary and cumulatively step upstream through the profile until the total distance is equal to the knickpoint travel distance, x. The difference between the calculated travel times through that distance and the initiation time (4.4 Ma) is the resulting misfit. The two-parameter exhaustive search approach applied searches parameter space linearly for values of m between 0.1 and 1.0 and logarithmically for K between 10^{-4} and 10^{-12}, to identify the best combination of m and K that minimizes the misfit among the three tributaries (Berlin and Anderson, 2007; Crosby and Whipple, 2006). The residual-minimized m and K for these tributaries are 0.42 and 9.33×10^{-7} $\mathrm{m}^{-0.16}\,\mathrm{yr}^{-1}$ respectively.

We applied these best-fit values of m and K using the celerity equation in a forward sense to the Yarlung main channel to predict the location of the Jiacha knickpoint as a function of time. The Jiacha knickpoint projects back in time to the base of the three modeled tributaries (Fig. 3) at 4.4 Ma which is consistent with the notion that the tributary knickpoints were formed by migration of the Jiacha knickpoint. Following the same approach, the Jiacha

knickpoint projects just upstream of the Namche Barwa massif at ~10 Ma (Fig. 3) and migrated at an average rate of ~40 km/Ma.

5. Thermokinematic modeling

Our bulk apatite ages, ^{4}He/^{3}He-based thermal histories, and celerity modeling suggest that a wave of incision migrated through the Yarlung River valley from the Namche Barwa massif starting at ~10 Ma. We use a forward 3D thermokinematic model to evaluate geologically plausible incision scenarios consistent with our observed apatite (U–Th)/He data (using a modified version of Pecube; Braun, 2003). For a prescribed model of topographic evolution, the model solves the heat transport equation through time incorporating variable kinematic parameters to predict time–temperature history of each node in a 3-dimensional grid.

Models of canyon incision require integrating both vertical background surface erosion and the development of topography through time. As an initial condition of the model, we create a simplified topography to simulate a flat surface cut by a 1.5 km deep valley with an 80 km long knickpoint (Fig. S5). With successive time steps, the knickpoint advances horizontally upstream to cut the valley to a total of 2 km deep. The background erosion rate, and its variance through time, is a prescribed parameter in our model, as are knickpoint migration rate and geothermal gradient. We explored the effects of broadly varying each parameter on the time–temperature history of the downstream canyon. Prescribed knickpoint retreat rates dictate the model run times and we varied these between 15–35 km/Ma. We assigned typical geothermal gradients of either 25 °C/km or 30 °C/km. High-elevation (U–Th)/He apatite ages from near the Yarlung–Nyang confluence indicate background exhumation rates are on the order of 0.25 km/Ma (Zeitler et al., 2014). However, we explored an order of magnitude variation in background erosion rates possible in this region by assigning it to be either 0.01 km/Ma or 0.25–0.2 km/Ma.

For each model run, we extracted time–temperature paths for nodes downstream of the ending knickpoint location that correspond to our sample location distance from the Jiacha knickpoint. We then use HeFTy (Ketcham, 2005) to predict apatite (U–Th)/He ages for the t–T paths of each of the five sample nodes, assuming ^{4}He diffusion kinetics prescribed by the radiation damage accumulation and annealing model (RDAAM; Flowers et al., 2009). We then calculated the sum of squared residuals between the predicted and observed (U–Th)/He ages for each model run, and use its minimum to identify the best fitting of the explored Pecube models (Table S4).

We find that a knickpoint retreat rate of 30 km/Ma succeeds in predicting the youngest (U–Th)/He ages and an increasing trend with downstream distance (Fig. 6), assuming a geothermal gradient of 25 °C/km and a continuous background exhumation rate of 0.2 km/Ma. Models with much faster rates of retreat predict apatite (U–Th)/He ages far younger than those observed and those with prescribed background erosion rates an order of magnitude slower predict (U–Th)/He ages that are far older.

6. Discussion

Our results indicate that the geomorphic evolution of the Yarlung River and therefore erosion in southern Tibet between the Namche Barwa Massif and the Jiacha knickpoint has been influenced by a downstream base level fall in the Late Miocene. Furthermore, our data provide insights into the evolution of the drainage network surrounding the eastern Himalayan Syntaxis. Finally, we examine major river profiles in eastern Tibet to explore proposed river capture models for this region and speculate on the origin of the Jiacha knickpoint.

6.1. Timing of knickpoint retreat in the upper Yarlung valley

In our knickpoint celerity model, the time at which the three modeled tributaries experienced a base level fall is assumed to be roughly 4.4 Ma (t). This is based on the closest apatite ^{4}He/^{3}He sample affected by knickpoint migration (sample ML01). In this model, the Jiacha knickpoint projects to the upstream edge of the Namche Barwa massif at ~10 Ma. Solutions to the knickpoint celerity model are linear, meaning that a doubling of the assumed initiation time for the tributary knickpoints to 8.8 Ma relocates the Jiacha knickpoint to this point at ~20 Ma. We find that scenarios where t is far less than 4.4 Ma predict past locations that are inconsistent with our ^{4}He/^{3}He apatite data. Apatite (U–Th)/He ages of 7–12 Ma downstream of our sample locations (Zeitler et al., 2014) are also consistent with propagation of the Jiacha knickpoint over ~10 Ma.

Knickpoint retreat rates derived from our interpretation of ^{4}He/^{3}He apatite spectra and (U–Th)/He ages are 20–25 km/Ma. Our celerity modeling results suggest rates of ~40 km/Ma, whereas the best-fitting Pecube result was modeled with a retreat rate of 30 km/Ma. Although there is a degree of dependence of the celerity modeling on the apatite data, given the uncertainty in these analyses, the rates calculated among the different methods do not vastly differ and highlight the consistency of our model predictions. The discrepancy between retreat rates predicted from the thermokinematic and celerity modeling are likely due to the simplified nature of this application of Pecube, which does not include a full landscape evolution model.

The best fitting of the explored Pecube models predicts ages for the three samples farthest downstream that are slightly too young when compared to our observed data. This may result from these samples having been collected from valley-wall locations that do not accurately represent paleo-river level. Wang et al. (2014) demonstrated that the bedrock river valley is buried beneath ~500 m of sediment in this portion of the Yarlung. Samples collected from 500 m above river level would produce ages that were slightly too old for our given model assumptions.

Collectively, the results presented here demonstrate that the knickpoints at ~3500 m are present throughout the present-day Yarlung River drainage network and that a wave of incision migrated westward upstream from the western border of the Namche Barwa massif. This indicates that the base level fall that formed the Jiacha knickpoint occurred downstream along the present course of the Yarlung River and that the Yarlung has flowed eastward along the Indus–Yarlung suture from Jiacha through the Eastern Syntaxis since at least ~10 Ma. This interpretation and the findings of Lang and Huntington (2014) contrast with the idea that the Yarlung River flowed westward through the Himalaya-traversing Subansiri River for any significant amount of time (Cina et al., 2009; Zhang et al., 2012). Notwithstanding, short-duration glacial or landslide damming events on the Yarlung River (see Korup and Montgomery, 2008; Montgomery et al., 2004) may have temporarily impeded eastward flow and retreat of the knickpoint and forced intermittent trans-Himalayan routing.

Apatite (U–Th)/He and fission track ages from farther downstream near the Nyang confluence decrease to 4–5 Ma and within the Yarlung gorge are <1 Ma (Seward and Burg, 2008; Zeitler et al., 2014). Young apatites outside of the massif are likely affected by lateral heat flow, which advects isotherms towards the surface (Zeitler et al., 2014); consequently any evidence of knickpoint migration directly adjacent to the massif has been removed. Recent discussion regarding tectonic-erosional feedbacks in this region suggests that incision of the Yarlung promotes rapid rock uplift in the massif that began at 8–10 Ma (Zeitler et al., 2014). As localized rapid exhumation progressed, the position of the large ~2 km knickpoint within the Namche Barwa massif was fixed, holding

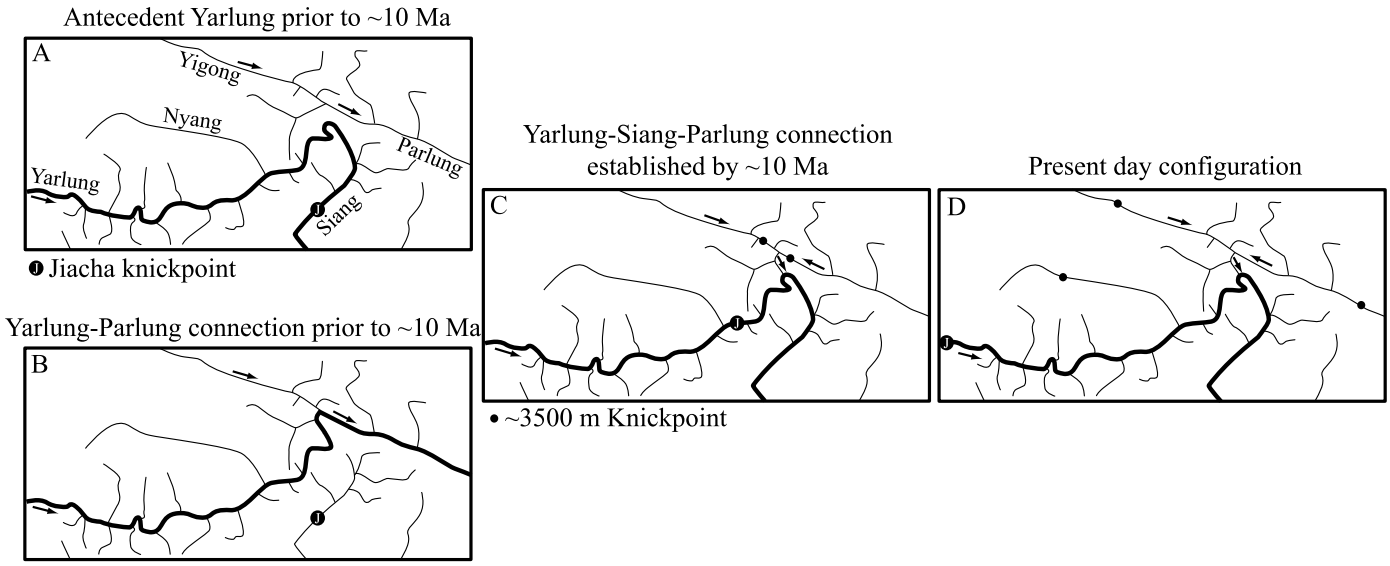

Fig. 7. Schematic temporal progression of Yarlung–Parlung–Siang integration scenarios consistent with present day knickpoint locations. Unlabeled tributaries are those analyzed here that contain knickpoints at ~3500 m. Black circles are locations of ~3500 m elevation knickpoints on major rivers of the region. Black arrows depict flow directions. Panels A, C, and D demonstrate an antecedent Yarlung–Siang drainage captures the Parlung prior to migration of the Jiacha knickpoint from the Siang. Panels B, C, and D show a similar scenario with a Yarlung–Parlung drainage prior to its capture by a headward-cutting Siang. Regardless of pre-integration configuration, integration by ~10 Ma is required to account for Parlung and tributary knickpoints.

upstream base level to ~3000 m, which is consistent with a slowing of upstream erosion rates after 5 Ma (Finnegan et al., 2008; Zeitler et al., 2014). Our calculated retreat rates suggest the Jiacha knickpoint migrated out of the massif just prior to or coincident with the initiation of rapid rock uplift. It is interesting to note this nearly synchronous series of events and we speculate on a relationship between knickpoint migration and initiation of rapid rock uplift in the syntaxis in Section 6.3. Our knickpoint migration model is consistent with recent measurement of an ~500 m thick sediment package within the Yarlung River downstream of the Jiacha knickpoint (Wang et al., 2014) in that our apatite data and knickpoint celerity modeling require the river to occupy a deeply incised canyon that formed over the last ~10 Ma. Formation of the ~2 km knickpoint within the Yarlung gorge and backfilling of the Yarlung canyon however may have initiated anytime between 2.5 Ma (Wang et al., 2014) and ~10 Ma.

6.2. Implications for drainage evolution

Barbed tributaries and wind gaps along the Parlung River indicate that it once flowed to the southeast through the Lhuit and/or Irrawaddy Rivers, contrasting its present-day northwest flow direction (Fig. 3; Burchfiel et al., 2000; Clark et al., 2004). Two end-member models for the reversal of the Parlung suggest very different paleo-drainage patterns within the region and thus different sediment evacuation routes. Some authors have postulated the existence of an antecedent Yarlung–Siang–Brahmaputra River, flowing in its present configuration since at least the Early Miocene (Fig. 7A), with capture of a separate Yigong–Parlung–Lhuit River occurring by northeastward migration of the deforming Namche Barwa antiform (Hallet and Molnar, 2001; Lang and Huntington, 2014; Seward and Burg, 2008). Others suggest a paleo-Yarlung–Parlung–Lhuit connection with headward cutting of the Siang–Brahmaputra capturing the Parlung (Fig. 7B; Brookfield, 1998; Clark et al., 2004; Liang et al., 2008; Robinson et al., 2014).

Our results provide new perspective on the timing of these drainage integration models just east of the Namche Barwa area. Long profiles and slope-area analysis of the Siang, Parlung, and Yigong rivers and their tributaries highlight the presence of ~3500 m elevation knickpoints (Fig. 3) indicating that these rivers have experienced the same base level fall as the Yarlung River. Based on these observations, we constrain knickpoint migration pathways and the timing of previously proposed scenarios for river reorganization consistent with the locations of knickpoints at ~3500 m in the drainage network.

If integration of the Yarlung, Parlung, and Siang occurred after the Jiacha knickpoint reached the upper Yarlung valley, both the Siang–Brahmaputra and the Parlung–Lhuit would have experienced this base level fall independently as we find evidence for knickpoints at ~3500 m elevation in both drainages. In a model in which the Yarlung was connected to the Parlung–Lhuit prior to this integration, the Jiacha knickpoint would have traveled up the Lhuit, through the Parlung, and into the upper Yarlung valley. However, we find evidence of an ~3500 m elevation knickpoint in the Parlung longitudinal profile presently located upstream of tributaries also containing knickpoints at ~3500 m elevation, indicating the Parlung knickpoint propagated from the northwest. If it had migrated from the southeast, we would not expect to find ~3500 m elevation knickpoints on tributaries that meet the Parlung northwest of the present day Parlung knickpoint (Fig. 3). This suggests that the Parlung has flowed in its present northwesterly course since at least ~10 Ma, which is inconsistent with a post-10 Ma integration scenario. In an antecedent Yarlung–Siang–Brahmaputra model, the Jiacha knickpoint would have originated on the Siang or Brahmaputra portion of the drainage. The ~3500 m elevation knickpoints on the tributaries of the Parlung and Yigong would therefore be the result of the same base level fall but would have originated on the Lhuit rather than the Siang or Brahmaputra. An early connection between the Yarlung and Siang–Brahmaputra is consistent with Gangdese detritus in Miocene foreland units (Cina et al., 2009; Lang and Huntington, 2014). However, the location of the Parlung knickpoint is again inconsistent with migration from the Lhuit.

We note that the Lhuit does not contain a major knickpoint at ~3500 m and acknowledge that after Jiacha knickpoint migration, localized uplift of the Parlung–Lhuit wind gap could have obscured evidence of it. This would suggest that the Parlung knickpoint did not result from the base level fall discussed in this paper, but rather represents a later knickpoint that was subsequently uplifted

to ~3500 m. However, we are presently unaware of any evidence for such localized uplift in this region.

If integration of the Yarlung, Parlung, and Siang rivers occurred prior to ~10 Ma, the Jiacha knickpoint would have originated from within the Siang or Brahmaputra portion of the drainage (Fig. 7A, B). This is consistent with knickpoints at ~3500 m elevation present within tributaries of the Siang, close to its confluence with the Yarlung. Gangdese Batholith-derived detritus present within Early through Late Miocene units of the Himalayan foreland basin is also consistent with pre-Late Miocene connection of the Yarlung and Siang–Brahmaputra (Chirouze et al., 2013; Cina et al., 2009; Lang and Huntington, 2014). Moreover, evidence of fish species diversification at 19–24 Ma (Britz, 2009; Rüber et al., 2004) and an increase in sediment flux into the Bengal Basin in the Eocene to Early Miocene (Alam et al., 2003) indicate an early capture event as suggested by Robinson et al. (2014).

Because knickpoints at ~3500 m elevation exist on both the Parlung and Yigong rivers and evidence of uplift in the Parlung–Lhuit wind gap is lacking, these knickpoints likely migrated up the Parlung and Yigong via the Siang. This requires that the Yarlung, Yigong, Parlung, and Siang were integrated at the time of headward migration through the Namche Barwa region. In this case, either pre-integration drainage configuration previously proposed is consistent with the mapped knickpoint locations, as long as integration occurred prior to ~10 Ma (Fig. 7).

6.3. Origin of 3500 m elevation knickpoint

From our knickpoint mapping, we infer that a major base level fall occurred downstream of the Yarlung–Siang confluence that caused knickpoint formation and generated a wave of incision that propagated upstream as previously suggested by Zeitler et al. (2014). We find evidence of this base level fall in knickpoints in tributaries on the Siang downstream until the maximum elevations of its tributaries do not reach 3500 m. Below this point, the tributaries may have experienced a base level fall, but the stream has fully adjusted to the new base level, precluding preservation and observation of a knickpoint.

A base level fall could be the result of a drainage capture event, deformation or uplift, or an abrupt change in precipitation. However, knickpoints at ~3500 m elevation are evident on other major rivers on the eastern margin of the Tibetan plateau including the Irrawaddy, Salween, Mekong, Yangtze, and Yalong (Fig. S1). Harkins et al. (2007) also describe a knickpoint at ~3500 m elevation on the Yellow river and several of its tributaries. Given the elevation change at the Jiacha knickpoint is 500 m, and that we find knickpoints of its approximate elevation throughout the eastern Tibetan plateau, we speculate that these knickpoints resulted from uplift of at least 500 m of the entire eastern margin just prior to ~10 Ma. Clark et al. (2005) and Duvall et al. (2012) describe a similar wave of incision at 9–13 Ma constrained by apatite (U–Th)/He thermochronology in the three-rivers region and elsewhere on the eastern margin of Tibet, which they relate to eastward expansion of the plateau. Additional knickpoint celerity modeling and thermochronologic constraints on the rivers of eastern Tibet are required to address the scale and potential synchronicity of this base level change.

Localized rapid rock uplift within the Namche Barwa massif pinned an ~2 km knickpoint to this location (Zeitler et al., 2001; Koons et al., 2013). As our celerity modeling suggests, the Jiacha knickpoint migrated out of this region at ~10 Ma, concurrent with or just prior to development of rapid rock uplift (Zeitler et al., 2014). The Jiacha and Namche Barwa knickpoints may have originated as a single feature resulting from a base level fall and were segmented with pinning of the Namche Barwa knickpoint. A 500 m elevation change (i.e. the Jiacha knickpoint) continued to migrate upstream to its present position. If resulting from the uplift of the southeastern margin of Tibet just prior to ~10 Ma, the full magnitude of this base level fall may have been the combined elevation change of these two features. Total uplift of the margin could therefore be upwards of 2.5 km.

7. Conclusions

We present thermochronology, knickpoint celerity modeling, and thermokinematic modeling from southeastern Tibet that demonstrates the mechanism and timing of incision of the Yarlung River. A series of ~3500 m elevation knickpoints exists throughout the region and slope-area and χ analysis of several longitudinal profiles from the drainage basin confirms their genetic relationship, suggesting a wave of knickpoint migration incised the Yarlung canyon. ^{4}He/^{3}He apatite thermochronology data from transect along the Yarlung are consistent with a wave of incision propagating upstream towards the Jiacha knickpoint. Celerity modeling projects the Jiacha knickpoint to just upstream of the Namche Barwa massif at ~10 Ma. Thermokinematic modeling of a simplified Jiacha knickpoint incision scenario predicts apatite (U–Th)/He ages similar to our observed data.

The spatial arrangement of multiple knickpoints at ~3500 m elevation in this region indicates that previously-recognized reorganization of the major rivers in the drainage just east of the Namche Barwa massif occurred prior to ~10 Ma and that the Yarlung flowed predominantly eastward since at least this time. Our results suggest a major base level fall resulting from uplift of 500–2500 m of the southeastern Tibetan margin occurred just prior to ~10 Ma.

Acknowledgements

This work was supported by an NSF Continental Dynamics program grant (EAR-1111853) to P.K.Z. and D.L.S. and a Geological Society of America Graduate Student Research Grant to J.L.S. We thank Fanyi Meng, Jin Yue, and Yue Chen for collecting and sharing samples and Zhidan Zhao, Mo Xuanxue, and Di-Cheng Zhu for help with field logistics.

Appendix A. Supplementary material

Supplementary material related to this article can be found online at http://dx.doi.org/10.1016/j.epsl.2015.08.041.

References

Alam, M., Alam, M.M., Curray, J.R., Chowdhury, M.L.R., Gani, M.R., 2003. An overview of the sedimentary geology of the Bengal Basin in relation to the regional tectonic framework and basin-fill history. Sediment. Geol. 155, 179–208.

Berlin, M.M., Anderson, R.S., 2007. Modeling of knickpoint retreat on the Roan Plateau, western Colorado. J. Geophys. Res. 112, F03S06.

Braun, J., 2002. Quantifying the effect of Recent relief changes on age-elevation relationships. Earth Planet. Sci. Lett. 200, 331–343.

Braun, J., 2003. Pecube; a new finite-element code to solve the 3D heat transport equation including the effects of a time-varying, finite amplitude surface topography. Comput. Geosci. 29, 787–794.

Britz, R., 2009. Danionella priapus, a new species of miniature cyprinid fish from West Bengal, India (Teleostei: Cypriniformes: Cyprinidae). Zootaxa, 53–60.

Brookfield, M.E., 1998. The evolution of the great river systems of southern Asia during the Cenozoic India–Asia collision; rivers draining southwards. Geomorphology 22, 285–312.

Burchfiel, B.C., Clark, M., Wang, E., Chen, Z., Liu, Y., Pan, G., 2000. Tectonic framework of the Namche Barwa region, Eastern Himalayan Syntaxis, SE Tibet. Abstr. Program – Geol. Soc. Am. 32, 33.

Chirouze, F., Huyghe, P., van der Beek, P., Chauvel, C., Chakraborty, T., Dupont-Nivet, G., Bernet, M., 2013. Tectonics, exhumation, and drainage evolution of the eastern Himalaya since 13 Ma from detrital geochemistry and thermochronology, Kameng River section, Arunachal Pradesh. Geol. Soc. Am. Bull. 125, 523–538.

Cina, S., Yin, A., Grove, M., Dubey, C., Shukla, D., Lovera, O., Kelty, T., Gehrels, G., Foster, D., 2009. Gangdese arc detritus within the eastern Himalayan Neogene

foreland basin: implications for the Neogene evolution of the Yalu–Brahmaputra River system. Earth Planet. Sci. Lett. 285, 150–162.
Clark, M.K., House, M.A., Royden, L.H., Whipple, K.X., Burchfiel, B.C., Zhang, X., Tang, W., 2005. Late Cenozoic uplift of southeastern Tibet. Geology 33, 525–528.
Clark, M.K., Schoenbohm, L.M., Royden, L.H., Whipple, K.X., Burchfiel, B.C., Zhang, X., Tang, W., Wang, E., Chen, L., 2004. Surface uplift, tectonics, and erosion of eastern Tibet from large-scale drainage patterns. Tectonics 23, 20.
Crosby, B.T., Whipple, K.X., 2006. Knickpoint initiation and distribution within fluvial networks; 236 waterfalls in the Waipaoa River, North Island, New Zealand. Geomorphology 82, 16–38.
Duvall, A.R., Clark, M.K., Avdeev, B., Farley, K.A., Chen, Z., 2012. Widespread late Cenozoic increase in erosion rates across the interior of eastern Tibet constrained by detrital low temperature thermochronometry. Tectonics 31, TC3014.
Finnegan, N.J., Hallet, B., Montgomery, D.R., Zeitler, P.K., Stone, J.O., Anders, A.M., Liu, Yuping, 2008. Coupling of rock uplift and river incision in the Namche Barwa–Gyala Peri Massif, Tibet. Geol. Soc. Am. Bull. 120, 142–155.
Flowers, R.M., Ketcham, R.A., Shuster, D.L., Farley, K.A., 2009. Apatite (U–Th)/He thermochronometry using a radiation damage accumulation and annealing model. Geochim. Cosmochim. Acta 73, 2347–2365.
Goren, L., Fox, M., Willett, S.D., 2014. Tectonics from fluvial topography using formal linear inversion; theory and applications to the Inyo Mountains, California. J. Geophys. Res., Earth Surf. 119, 1651–1681.
Hack, J.T., 1957. Studies of longitudinal stream profiles in Virginia and Maryland. In: U.S. Geological Survey Professional Paper, pp. 45–97.
Hallet, B., Molnar, P., 2001. Distorted drainage basins as markers of crustal strain east of the Himalaya. J. Geophys. Res. 106, 13–13,709.
Harkins, N., Kirby, E., Heimsath, A., Robinson, R., Reiser, U., 2007. Transient fluvial incision in the headwaters of the Yellow River, northeastern Tibet, China. J. Geophys. Res. 112, F03S04.
Howard, A.D., 1994. A detachment-limited model of drainage basin evolution. Water Resour. Res. 30, 2261–2285.
Howard, A.D., Kerby, G., 1983. Channel changes in badlands. Geol. Soc. Am. Bull. 94, 739–752.
Kapp, P., Guynn, J.H., 2004. Indian punch rifts Tibet. Geology 32, 993–996.
Kapp, P., Taylor, M., Stockli, D., Ding, L., 2008. Development of active low-angle normal fault systems during orogenic collapse; insight from Tibet. Geology 36, 7–10.
Ketcham, R.A., 2005. Forward and inverse modeling of low-temperature thermochronometry data. Rev. Mineral. Geochem. 58, 275–314.
Kirby, E., Whipple, K., 2001. Quantifying differential rock-uplift rates via stream profile analysis. Geology 29, 415–418.
Koons, P.O., Zeitler, P.K., Hallet, B., 2013. Tectonic aneurysms and mountain building. In: Schroder, J., Owen, L.A. (Eds.), Treatise on Geomorphology. Academic Press, San Diego, pp. 318–349.
Korup, O., Montgomery, D.R., 2008. Tibetan plateau river incision inhibited by glacial stabilization of the Tsangpo gorge. Nature 455, 786–789.
Lang, K.A., Huntington, K.W., 2014. Antecedence of the Yarlung–Siang–Brahmaputra River, eastern Himalaya. Earth Planet. Sci. Lett. 397, 145–158.
Liang, Y., Chung, S., Liu, D., Xu, Y., Wu, F., Yang, J., Wang, Y., Lo, C., 2008. Detrital zircon evidence from Burma for reorganization of the eastern Himalayan river system. Am. J. Sci. 308, 618–638.
Mancktelow, N.S., Grasemann, B., 1997. Time-dependent effects of heat advection and topography on cooling histories during erosion. Tectonophysics 270, 167–195.
Montgomery, D.R., Hallet, B., Liu, Y., Finnegan, N., Anders, A., Gillespie, A., Greenberg, H.M., 2004. Evidence for Holocene megafloods down the Tsangpo River gorge, southeastern Tibet. Quat. Res. 62, 201–207.
Niemann, J.D., Gasparini, N.M., Tucker, G.E., Bras, R.L., 2001. A quantitative evaluation of Playfair's law and its use in testing long-term stream erosion models. Earth Surf. Process. Landf. 26, 1317–1332.
Perron, J.T., Royden, L., 2013. An integral approach to bedrock river profile analysis. Earth Surf. Process. Landf. 38, 570–576.
Pritchard, D., Roberts, G.G., White, N.J., Richardson, C.N., 2009. Uplift histories from river profiles. Geophys. Res. Lett. 36.
Robinson, R.A.J., Brezina, C.A., Parrish, R.R., Horstwood, M.S.A., Oo, N.W., Bird, M.I., Thein, M., Walters, A.S., Oliver, G.J.H., Zaw, K., 2014. Large rivers and orogens; the evolution of the Yarlung Tsangpo–Irrawaddy system and the eastern Himalayan syntaxis. Gondwana Res. 26, 112–121.
Rosenbloom, N.A., Anderson, R.S., 1994. Hillslope and channel evolution in a marine terraced landscape, Santa Cruz, California. J. Geophys. Res. 99, 13–14,029.
Royden, L., Perron, J.T., 2013. Solutions of the stream power equation and application to the evolution of river longitudinal profiles. J. Geophys. Res., Earth Surf. 118, 497–518.
Rüber, L., Britz, R., Kullander, S.O., Zardoya, R., 2004. Evolutionary and biogeographic patterns of the Badidae (Teleostei: Perciformes) inferred from mitochondrial and nuclear DNA sequence data. Mol. Phylogenet. Evol. 32, 1010–1022.
Schildgen, T.F., Balco, G., Shuster, D.L., 2010. Canyon incision and knickpoint propagation recorded by apatite $^{4}He/^{3}He$ thermochronometry. Earth Planet. Sci. Lett. 293, 377–387.
Seward, D., Burg, J.P., 2008. Growth of the Namche Barwa Syntaxis and associated evolution of the Tsangpo Gorge; constraints from structural and thermochronological data. Tectonophysics 451, 282–289.
Shuster, D.L., Cuffey, K.M., Sanders, J.W., Balco, G., 2011. Thermochronometry reveals headward propagation of erosion in an alpine landscape. Science 332, 84–88.
Shuster, D.L., Farley, K.A., Sisterson, J.M., Burnett, D.S., 2004. Quantifying the diffusion kinetics and spatial distributions of radiogenic ^{4}He in minerals containing proton-induced ^{3}He. Earth Planet. Sci. Lett. 217, 19–32.
Shuster, D.L., Flowers, R.M., Farley, K.A., 2006. The influence of natural radiation damage on helium diffusion kinetics in apatite. Earth Planet. Sci. Lett. 249, 148–161.
Snyder, N.P., Whipple, K.X., Tucker, G.E., Merritts, D.J., 2000. Landscape response to tectonic forcing; digital elevation model analysis of stream profiles in the Mendocino triple junction region, Northern California. Geol. Soc. Am. Bull. 112, 1250–1263.
Stewart, R.J., Hallet, B., Zeitler, P.K., Malloy, M., Allen, C.M., Trippett, D., 2008. Brahmaputra sediment flux dominated by highly localized rapid erosion from the easternmost Himalaya. Geology 36, 711–714.
van der Beek, P., Bishop, P., 2003. Cenozoic river profile development in the upper Lachlan catchment (SE Australia) as a test of quantitative fluvial incision models. J. Geophys. Res. 108.
Wang, P., Scherler, D., Liu-Zeng, J., Mey, J., Avouac, J., Zhang, Y., Shi, D., 2014. Tectonic control of Yarlung Tsangpo Gorge revealed by a buried canyon in southern Tibet. Science 346, 978–981.
Weissel, J.K., Seidl, M.A., 1998. Inland propagation of erosional escarpments and river profile evolution across the Southeast Australian passive continental margin. In: Geophysical Monograph, vol. 107, pp. 189–206.
Whipple, K.X., Hancock, G.S., Anderson, R.S., 2000. River incision into bedrock; mechanics and relative efficacy of plucking, abrasion, and cavitation. Geol. Soc. Am. Bull. 112, 490–503.
Whipple, K.X., Tucker, G.E., 1999. Dynamics of the stream-power river incision model; implications for height limits of mountain ranges, landscape response timescales, and research needs. J. Geophys. Res. 104, 17–17,674.
Yin, A., Kapp, P.A., Murphy, M.A., Manning, C.E., Harrison, T.M., Grove, M., Ding, L., Deng, X., Wu, C., 1999. Significant late Neogene east–west extension in northern Tibet. Geology 27, 787–790.
Yin, A., Dubey, C.S., Kelty, T.K., Webb, A.A.G., Harrison, T.M., Chou, C.Y., Célérier, J., 2010. Geologic correlation of the Himalayan orogen and Indian craton: Part 2. Structural geology, geochronology, and tectonic evolution of the Eastern Himalaya. Geol. Soc. Am. Bull. 122, 360–395.
Zaprowski, B.J., Evenson, E.B., Pazzaglia, F.J., Epstein, J.B., 2001. Knickzone propagation in the Black Hills and northern High Plains; a different perspective on the late Cenozoic exhumation of the Laramide Rocky Mountains. Geology 29, 547–550.
Zeitler, P.K., Meltzer, A.S., Koons, P.O., Craw, D., Hallet, B., Chamberlain, C.P., Kidd, W.S.F., Park, S.K., Seeber, L., Bishop, M., Shroder, J., 2001. Erosion, Himalayan geodynamics, and the geomorphology of metamorphism. GSA Today 11, 4–9.
Zeitler, P.K., Meltzer, A.S., Brown, L., Kidd, W.S.F., Lim, C., Enkelmann, E., 2014. Tectonics and topographic evolution of Namche Barwa and the easternmost Lhasa Block, Tibet. In: Special Paper – Geological Society of America, vol. 507, pp. 23–58.
Zhang, D.D., 1998. Geomorphological problems of the middle reaches of the Tsangpo River, Tibet. Earth Surf. Process. Landf. 23, 889–903.
Zhang, J., Yin, A., Liu, W.C., Wu, F.Y., Lin, D., Grove, M., 2012. Coupled U–Pb dating and Hf isotopic analysis of detrital zircon of modern river sand from the Yalu River (Yarlung Tsangpo) drainage system in southern Tibet; constraints on the transport processes and evolution of Himalayan rivers. Geol. Soc. Am. Bull. 124, 1449–1473.